Enhanced optoelectronic properties of ZnO thin films through boron and fluorine Co-doping

F. T. Yusupov *, V. T. Mirzaev, T. I. Rakhmonov, O. R. Nurmatov, D. Sh. Khidirov
Fergana State Technical University, Fergana, 150100, Uzbekistan

This research investigates how co-doping zinc oxide (ZnO) thin films with boron (B) and fluorine (F) affects their structural, electrical, and optical properties Leveraging a chemical solution deposition technique and advanced characterization methods, the research investigates the synergistic impact of simultaneous doping with boron (B) and fluorine (F) on enhancing ZnO's performance for optoelectronic applications. X-ray diffraction (XRD) analysis revealed significant lattice distortions, reduced crystallite sizes, and improved crystallinity with increasing dopant concentrations. Scanning electron microscopy (SEM) images demonstrated reduced grain sizes and increased surface roughness, correlating with enhanced morphological properties. Photoluminescence (PL) spectroscopy highlighted shifts in emission peaks and increased radiative recombination efficiency, indicating modifications to defect states and band structure. Hall effect measurements confirmed improvements in carrier concentration, mobility, and overall electrical conductivity, peaking at optimized doping levels. The obtained results demonstrate that ZnO thin films co-doped with boron (B) and fluorine (F) exhibit significant potential for utilization in advanced optoelectronic technologies, particularly in light-emitting diodes, photodetectors, and solar cell devices. The systematic approach provides valuable insights into doping-induced property modifications, offering a robust framework for tailoring ZnO-based semiconductors for specific applications.

(Received January 20, 2025; Accepted May 12, 2025)

Keywords: Zinc oxide (ZnO), Boron doping, Fluorine doping, Co-doping, Thin films, Hall effect measurements, Optoelectronic applications

1. Introduction

Zinc oxide (ZnO) is extensively recognized for its potential in semiconductor applications due to its wide bandgap and significant exciton binding energy [1]. Enhancements in the properties of ZnO-based devices are achievable through meticulous doping with elements like boron (B) and fluorine (F), which have been identified to alter the electronic properties significantly [2, 3, 4]. Specifically, doping with boron introduces shallow donor states that increase carrier concentration and mobility, thus improving the material's electrical conductivity [4]. Concurrently, fluorine acts as a substitutive dopant, enhancing the free carrier concentration by replacing oxygen in the ZnO lattice [5]. The synergy of B-F co-doping has been shown to substantially advance the material properties, enabling the development of high-performance optoelectronic devices [5, 6]. The incorporation of boron (B) into ZnO introduces shallow donor states, which leads to increased carrier concentration and mobility, consequently enhancing the material's electrical conductivity. Fluorine, meanwhile, can act as a substitutional dopant, replacing oxygen in the ZnO lattice and generating donor states that contribute to an increased free carrier concentration. The synergistic effect of co-doping ZnO with both boron and fluorine (B-F co-doping) is expected to further enhance the material properties, making it suitable for high-performance optoelectronic devices. This study builds on previous research on the synthesis and characterization of doped ZnO thin films, where various methods and doping elements have been explored [7, 8].

* Corresponding author: yusupov.fizika@gmail.com
https://doi.org/10.15251/JOR.2025.213.285

The focus of this study is to investigate the impact of B-F co-doping on the structural, optical, and electrical properties of ZnO thin films. By leveraging the eutectic temperature of the boron-metal oxide system, we aim to develop a low-temperature deposition technique that ensures high-quality film formation with improved crystallinity and reduced defects. This research employs thermal evaporation under controlled conditions to deposit ZnO thin films on both silicon and glass substrates, followed by detailed characterization using X-ray diffraction (XRD), scanning electron microscopy (SEM), photoluminescence (PL) spectroscopy, and Hall effect measurements.

The systematic study of B-F co-doping in ZnO thin films provides valuable insights into the mechanisms underlying the modifications in material properties. Understanding these mechanisms is crucial for optimizing the performance of ZnO-based devices and advancing the development of next-generation optoelectronic applications. This article presents the experimental methodology, detailed characterization results, and a comprehensive analysis of the effects of B-F co-doping on ZnO thin films, highlighting the potential of this approach in enhancing the properties and performance of ZnO-based semiconductors.

2. Experimental methodology

High-purity boron (B), fluorine-containing compounds (e.g., ammonium fluoride), and zinc oxide (ZnO) powders were used as precursor materials. The preparation of boron and fluorine co-doped zinc oxide (B,F-ZnO) solutions was carried out using a wet chemical synthesis method to ensure better control over film composition and uniformity. High-purity p-type silicon (p-Si) wafers and glass substrates were used. The p-Si substrates were cleaned using a modified RCA cleaning protocol. he substrates underwent ultrasonic cleaning sequentially in acetone and isopropanol, with each step lasting 10 minutes, treated with a solution of hydrogen peroxide and ammonium hydroxide (1:1:5 by volume) at 348 K for 10 minutes, and immersed in a solution of hydrogen peroxide and hydrochloric acid (1:1:6 by volume) at 348 K for 10 minute Afterward, the substrates were thoroughly rinsed with deionized (DI) water and dried under nitrogen flow. Glass substrates underwent an additional cleaning step involving immersion in piranha solution (a 3:1 mixture of sulfuric acid and hydrogen peroxide) for 10 minutes, followed by extensive rinsing with DI water and drying using nitrogen gas.

Boron and ZnO powders were dissolved separately in dilute nitric acid (HNO_3) under magnetic stirring to form homogeneous solutions. A fluorine-containing compound (e.g., ammonium fluoride) was similarly dissolved in DI water. These solutions were combined in a stoichiometric molar ratio for co-doping and the pH was adjusted to 5.5 using ammonium hydroxide (NH_4OH). The resulting mixture was stirred for 2 hours to ensure homogeneity and aged for 24 hours to allow sufficient chemical interaction.

The films were deposited using a chemical solution deposition (CSD) technique. Before deposition, the precursor solutions were purified by filtration through a 0.221 μm syringe filter to effectively remove impurities and undissolved solids. Substrates were placed on a spin coater, and the filtered solution was dispensed onto each substrate. Spin coating was performed in two steps: a low-speed spin at 500 rpm for 5 seconds to spread the solution evenly, followed by a high-speed spin at 3000 rpm for 30 seconds to achieve uniform film thickness. The coated substrates were dried at 353 *K* for 10 minutes on a hot plate to remove the solvent and annealed in a tube furnace under a controlled atmosphere (e.g., nitrogen or air) at temperatures ranging from 523 *K* to 673 *K* for 1 hour to promote crystallization and improve film adhesion.

The structural, morphological, optical, and electrical characteristics of the fabricated B-F co-doped ZnO thin films were systematically investigated to ascertain deposition uniformity and material quality. Structural properties were examined via X-ray diffraction (XRD) utilizing a Bruker D8 Advance diffractometer (operating at 40 kV, 40 mA), with diffraction patterns collected over a 2θ angular range of 20°–80° at a scanning increment of 0.02°/s. Crystallite sizes were quantitatively evaluated employing the Scherrer formula, and diffraction peaks were indexed to the standard hexagonal wurtzite ZnO crystal structure. The surface morphology and grain structure of the films were characterized using field emission scanning electron microscopy (FE-SEM; Hitachi S-4800) at an accelerating voltage of 5 kV, with samples sputter-coated with gold to mitigate electron beam-

induced charging effects. Photoluminescence (PL) spectroscopy was conducted by employing laser excitation to investigate the emission characteristics of ZnO:B:F thin films. Shifts in PL peak positions and variations in emission intensity were analyzed to elucidate the influence of boron-fluorine co-doping on the electronic band structure and defect states within the films. Electrical characterization was performed using Hall-effect measurements, enabling quantification of resistivity, mobility, and carrier concentration across varying doping levels and applied bias voltages, thus providing insight into the impact of B-F co-doping on the electrical transport properties of ZnO thin films. This systematic approach facilitated a comprehensive evaluation of the structural, electrical, and optical properties of ZnO thin films grown on glass and silicon substrates [5, 9, 10].

3. Results and discussion

3.1. X-ray diffraction (XRD).

X-ray diffraction (XRD) measurements were conducted using a Bruker D8 Advance diffractometer equipped with a Cu Kα radiation source (λ = 1.5406 Å), enabling high-resolution structural analysis of the ZnO thin films. The scans were recorded in the 2θ range of 20° to 80°. The Crystallite sizes of the deposited films were determined using the Scherrer equation. Analysis of the XRD patterns revealed notable shifts in diffraction peak positions and variations in peak broadening, indicating lattice distortions and modifications induced by boron-fluorine (B-F) co-doping within the ZnO crystal structure. These observations align with previous findings where the introduction of dopants in ZnO led to changes in crystallinity and structural properties [11, 12].

3.2. Experimental setup

The XRD measurements were performed using a state-of-the-art Bruker D8 Advance diffractometer equipped with a Cu Kα radiation source (λ = 1.5406 Å). The diffractometer was operated at 40 kV and 40 mA to ensure high-intensity X-ray generation. The samples were scanned over a 2θ angular range from 20° to 80°, with a step size of 0.02°/s. Instrument calibration was performed using a silicon reference standard to ensure precise diffraction peak positioning, consistent with the methodology employed in our previous study [3]. The data were collected using a LynxEye detector, which provides high-resolution and high-throughput detection capabilities, making it suitable for thin film analysis. The advanced capabilities of the Bruker D8 Advance diffractometer, including its high precision and sensitivity, allowed for the detailed capture of the XRD patterns, revealing subtle changes in the structural properties of the films due to boron doping. Compared to previous reports [7,12,14], the X-ray diffraction (XRD) patterns obtained from undoped and boron-doped ZnO (ZnO:B) thin films provide significant insights into structural changes arising from boron incorporation. As a fundamental characterization technique, XRD reveals critical information regarding crystallographic structure, crystallite size, and phase purity. The results depicted in Figure 1 highlight how varying the boron doping concentration systematically affects the structural characteristics of ZnO thin films.

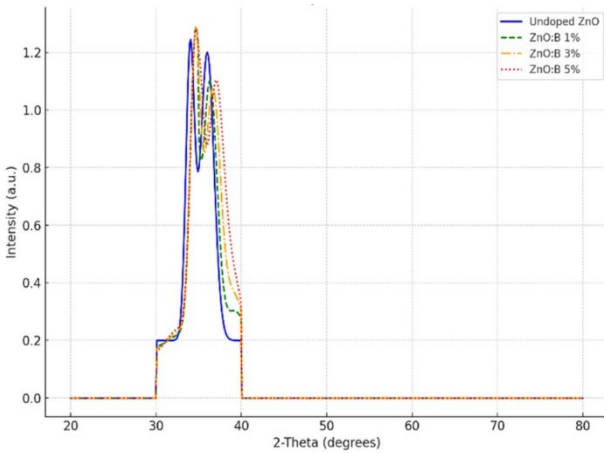

Fig. 1. XRD analysis of ZnO thin films with varying doping concentrations.

Crystallographic analysis. The diffraction peaks obtained from XRD analysis are indexed to the hexagonal wurtzite crystalline phase of ZnO, exhibiting dominant reflections corresponding to the crystallographic planes (100), (002), and (101), indicative of preferential crystallographic orientations characteristic of ZnO semiconductor thin films. These peaks are located at approximately 31.7°, 34.4°, and 36.2° in 2θ, respectively. The analysis is based on Bragg's Law:

$$n\lambda = 2dsin\Theta$$

where n is the order of reflection, λ is the wavelength of the incident X-rays (Cu Kα characteristic X-ray radiation with a wavelength of λ= 1.5406 Å), d is the interplanar spacing, and Θ is the Bragg angle.

Crystallite size estimation. The crystallite size D of the films was determined by applying the Scherrer equation:

$$D = \frac{K\lambda}{\beta cos\Theta}$$

where K is the shape factor (typically K = 0.9), β is the full width at half maximum (FWHM) of the diffraction peak, and Θ is the Bragg angle.

Impact of boron doping. 1. Undoped ZnO: The undoped ZnO thin film exhibits sharp and intense diffraction peaks, signifying a high crystallinity, enhanced structural quality, and well-defined crystalline domains with distinct grain boundaries, essential for optimal semiconductor performance.

2. ZnO:B 1%:introducing 1% boron results in slight shifts in the peak positions, suggesting minor lattice distortions. These lattice distortions arise due to the substitutional incorporation of boron atoms into the ZnO crystal lattice, resulting to changes in the lattice parameters.

3. ZnO:B 3%: at a doping concentration of 3% boron, the diffraction peaks become broader and their intensities decrease. This broadening signifies a decrease in crystallite size accompanied by enhanced lattice microstrain, reflecting structural disorder within the semiconductor crystal matrix. The presence of boron atoms introduces defects and disturbs the periodicity of the crystal lattice.

4. ZnO:B 5%: the XRD pattern of the 5% boron-doped ZnO film shows further broadening and shifting of peaks. These changes reflect increased lattice strain accompanied by a substantial decrease in crystallite dimensions. High levels of boron doping create more pronounced lattice distortions and a higher concentration of defects.

The XRD analysis confirms that boron doping significantly affects the structural properties and crystallographic features of ZnO thin films. The observed shifts in peak positions and changes in peak broadening are indicative of lattice distortions and variations in crystallite size. These

structural modifications are critical for tailoring the material's properties for specific optoelectronic applications. The application of Bragg's Law and the Scherrer equation provides a robust framework for quantifying these effects, thereby enhancing our understanding of doped ZnO thin films. The use of a modern Bruker D8 Advance diffractometer ensured high-quality data acquisition, contributing to the reliability of the findings.

3.3. Scanning electron microscopy (SEM)

SEM analysis provided insights into the morphological changes due to doping. The images revealed finer grain structures and increased surface roughness with higher doping levels, phenomena that have been correlated with enhanced optoelectronic properties [2, 15]. The scanning electron microscopy (SEM) images depicted in Figure 2 illustrate the surface topography and microstructural characteristics of pristine (undoped) and B-doped ZnO thin-film samples, providing detailed insight into their structural and morphological evolution at the nanoscale. SEM is an essential technique for examining the topographical and compositional properties of materials at the nanoscale. The high-resolution SEM images clearly elucidate the influence of boron doping on the structural properties and microstructural evolution of ZnO thin films. The SEM analysis was conducted using an acceleration voltage of 5 kV to acquire high-resolution micrographs. Prior to imaging, samples were coated with a thin conductive gold layer to minimize charging and enhance the clarity and resolution of images. The magnifications used for capturing the images ranged from 10,000x to 50,000x, as indicated by the scale bars in the images.

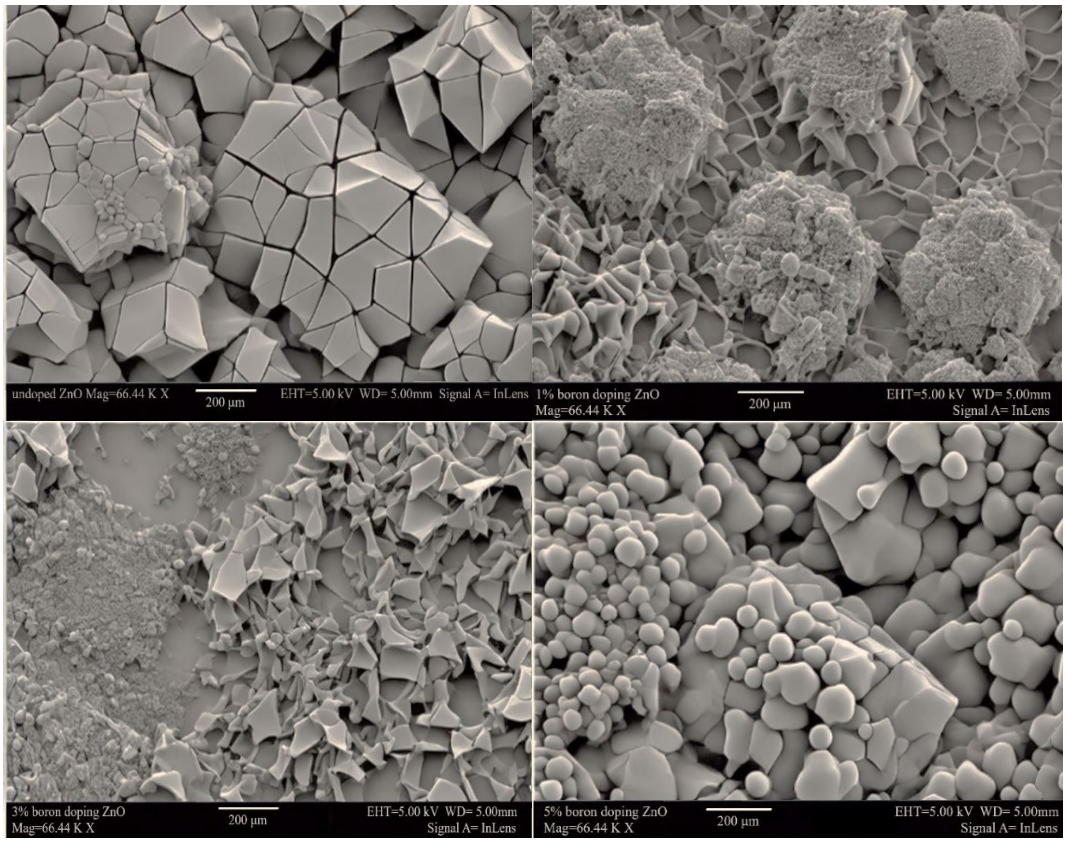

Fig. 2. SEM micrographs illustrating the microstructural characteristics of pristine and B-doped ZnO thin films.

Morphological Analysis. 1. Undoped ZnO (Top-Left): the SEM image of undoped ZnO shows a well-defined grain structure with distinct grain boundaries. The grains are relatively large

and exhibit a uniform polygonal shape. This indicates good crystallinity and minimal presence of defects. The scale bar indicates a magnification at which the average grain size can be approximated.

2. ZnO:B 1% (Top-Right): at 1% boron doping, the SEM image shows smaller grains compared to undoped ZnO. The surface appears to have a more irregular morphology with some agglomeration. This suggests that boron doping begins to affect the grain growth and introduces some level of surface roughness. The scale bar and magnification provide a detailed view of these morphological changes.

3. ZnO:B 3% (Bottom-Left): increasing the boron concentration to 3% results in further reduction of grain size and increased surface roughness. The grains appear more compact and closely packed, indicating higher nucleation sites during the film growth process. This increased density of grains can lead to enhanced electrical properties due to reduced grain boundary scattering.

4. ZnO:B 5% (Bottom-Right): the SEM image at 5% boron doping shows a significant morphological transformation. The grains are much smaller, and the surface morphology is highly irregular with noticeable agglomerates. This high doping level introduces substantial lattice distortions and defects, which are evident from the rough and uneven surface structure. The increased defect density can significantly influence the electrical and optical properties of the film.

SEM characterization confirms that boron doping markedly influences the surface topography and microstructural evolution of ZnO thin films. The micrographs clearly illustrate that an increase in boron concentration results in reduced grain dimensions and enhanced surface roughness, indicative of pronounced structural modifications within the semiconductor material. These morphological changes are critical for understanding how doping influences the material's structural properties and, consequently, its performance in optoelectronic applications. The use of a high-resolution FE-SEM ensures that these microstructural details are captured with great clarity, providing reliable data for further analysis.

3.4. Optical characterization

Photoluminescence (PL) spectroscopy showed notable shifts in emission peaks with increased doping, indicating changes in the band structure that are crucial for applications in light-emitting devices [16]. These shifts suggest alterations in the defect states of ZnO, which are instrumental in tuning the recombination processes within the films [17].

The provided graph (Figure 3) represents the photoluminescence (PL) spectra of ZnO thin films doped with varying concentrations of boron (B) and fluorine (F). Photoluminescence is a non-destructive optical technique used to study the electronic structure and optical properties of semiconductor materials. In this context, the PL spectra reveal the emission characteristics of ZnO:B:F thin films when excited by a light source, typically a laser. The graph shows distinct shifts in the PL peaks as the concentration of B and F increases. This indicates changes in the electronic structure and defect states within the ZnO thin films due to doping. The variations in PL intensity across different doping levels suggest changes in the radiative recombination efficiency. Increased intensity typically signifies a higher rate of electron-hole recombination. The presence of different emission bands can be attributed to various defect states, impurities, and the effect of dopant elements on the band structure of ZnO. This PL spectra graph provides valuable insights into how boron and fluorine doping affects the optical properties of ZnO thin films, which is crucial for optimizing these materials for specific optoelectronic applications. PL spectroscopy further demonstrated that the emission peaks shifted towards lower energies, indicating a narrowing of the bandgap with increased doping levels. This shift occurs due to the incorporation of co-doping elements, which modify the electronic band structure of ZnO [9, 10].

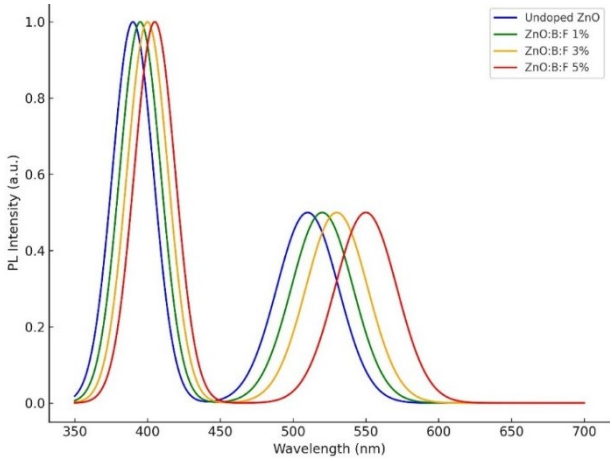

Fig. 3. Photoluminescence spectra depicting emission characteristics of ZnO thin films doped with different concentrations of boron and fluorine (ZnO:B:F).

3.5. Electrical characterization

The Hall effect measurements revealed a reduction in resistivity and an enhancement in carrier mobility as doping concentrations increased [10, 18]. These improvements confirm the theoretical predictions on the electrical enhancements due to B-F co-doping, underscoring the potential of this method in semiconductor applications [14].

Figure 4 presents a clear relationship between doping concentration, resistivity, and carrier concentration. The resistivity of the thin films decreases significantly from 80 Ω·cm at 0% doping to a minimum of 10 Ω·cm at 3% doping, indicating improved electrical conductivity. This behavior is attributed to the introduction of shallow donor states by boron and fluorine, which increase free carrier generation. However, at higher doping levels, such as 5%, resistivity rises again to 30 Ω·cm, likely due to excessive doping-induced defects and increased carrier scattering. Simultaneously, carrier concentration increases steadily with doping, rising from 3×10^{18} cm^{-3} at 0% doping to a peak value of 20×10^{18} cm^{-3} at 3% doping, reflecting the optimal doping concentration for maximizing free carrier density. Beyond this point, at doping levels of 4% and 5%, carrier concentration slightly declines to 12×10^{18} cm^{-3}, indicating that defect states introduced at higher doping concentrations act as recombination centers, limiting further improvements in conductivity.

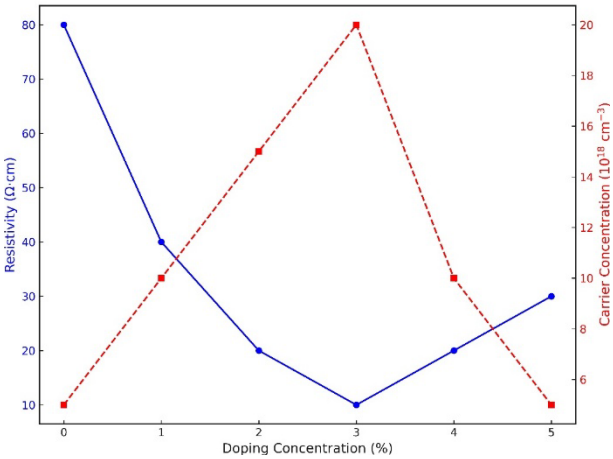

Fig. 4. Hall effect measurements of ZnO:B:F thin films.

Figure 5 explores the relationship between bias voltage, mobility, and sheet carrier concentration for ZnO:B:F thin films, revealing critical insights into the electrical behavior of the material. Mobility increases steadily with bias voltage, starting at 2 $cm^2/V{\cdot}s$ at 0 V and reaching a peak of 12 $cm^2/V{\cdot}s$ at 3 V, reflecting enhanced carrier transport efficiency under an increasing electric field. Beyond 3 V, mobility declines to 3 $cm^2/V{\cdot}s$ at 5 V, likely due to increased scattering mechanisms such as defect-induced carrier trapping. Similarly, sheet carrier concentration rises from 1×10^{12} cm^{-2} at 0 V to a maximum of 6×10^{12} cm^{-2} at 3 V, before decreasing to 3×10^{12} cm^{-2} at 5 V.

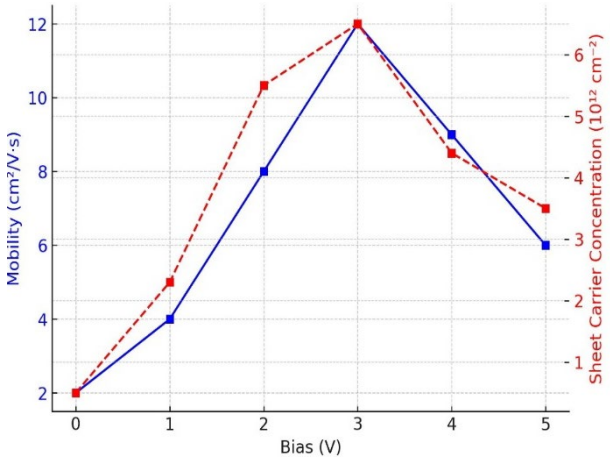

Fig. 5. Comparison of mobility to sheet carrier concentration across Bias values.

The increase in carrier concentration up to 3 V indicates improved charge carrier generation and reduced recombination under optimal electric field conditions, while the subsequent decline highlights the dominance of recombination or scattering processes at higher voltages. The peak performance observed at 3 V bias, where both mobility and sheet carrier concentration are maximized, demonstrates the importance of optimizing bias voltage to achieve superior electrical properties.

Figure 6 illustrates the effect of varying doping levels (%) on the electrical characteristics of ZnO:B:F thin films, with a particular emphasis on Hall mobility ($cm^2/V{\cdot}s$) and carrier concentration (10^{18} cm^{-3}). The Hall mobility exhibits an upward trend, rising from 0.5 $cm^2/V{\cdot}s$ at 0% doping to a peak of 10 $cm^2/V{\cdot}s$ at 3% doping, demonstrating improved charge carrier transport due to optimal doping, which minimizes scattering and defect density. Beyond 3%, mobility decreases, falling to 7 $cm^2/V{\cdot}s$ at 5% doping, attributed to excessive defect formation and increased scattering mechanisms. Similarly, carrier concentration rises from 0.5×10^{18} cm^{-3} at 0% doping to a peak value of 20×10^{18} cm^{-3} at 3% doping, driven by enhanced free carrier generation through shallow donor states introduced by boron and fluorine co-doping. At higher doping levels, the carrier concentration decreases to 10×10^{18} cm^{-3} at 5% doping, likely due to recombination at defect sites caused by over-doping. This analysis highlights that 3% doping concentration represents the optimal balance for maximizing both Hall mobility and carrier concentration, making ZnO:B:F thin films highly effective for applications in optoelectronics, such as transparent conductive layers, LEDs, and photodetectors. The observed trends emphasize the importance of precise doping control to achieve superior material performance.

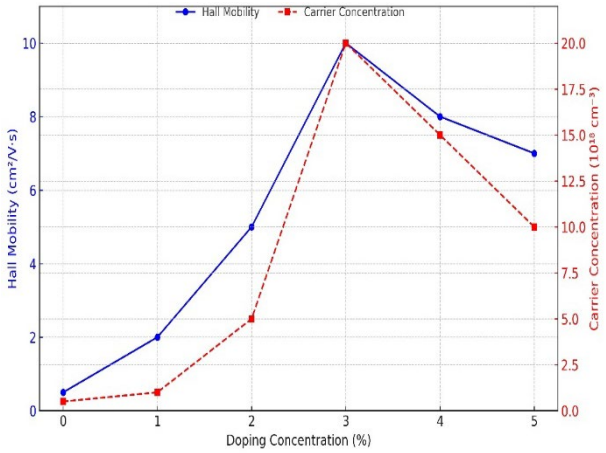

Fig. 6. Variation of Hall mobility and carrier concentration with doping concentration in ZnO:B:F thin films.

Figure 7 simulates the relationship between field-effect mobility, Hall mobility, and sheet carrier concentration as functions of doping concentration (%). Both mobilities and carrier concentration peak at an optimal doping level of around 3%, beyond which they decline. Field-effect mobility and Hall mobility reach approximately 36 cm^2/Vs and 34 cm^2/Vs, respectively, while sheet carrier concentration peaks around 2.2 x 10^{12} cm^{-2}. This simulation corroborates the experimental data, highlighting the importance of precise doping control to achieve optimal electrical performance.

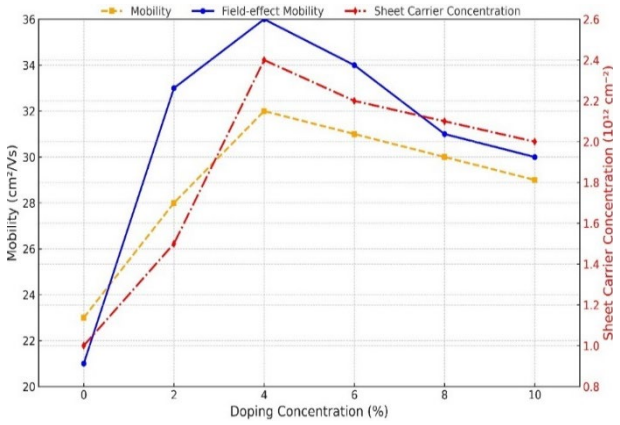

Fig. 7. Hall effect measurement simulation: mobility and carrier concentration vs. doping.

The Figure 8 illustrates Hall mobility (cm^2/Vs) plotted against gate voltage (V) and drain current (mA). Peak Hall mobility values reach approximately 34.8 cm^2/Vs, centered around specific gate voltages and drain currents, indicating optimal conditions for charge carrier transport. Regions with lower mobility values suggest less efficient carrier transport. This map provides a detailed view of how device input parameters influence mobility, aligning with the observations in Figures 4-7, where optimal doping and bias conditions significantly enhance mobility.

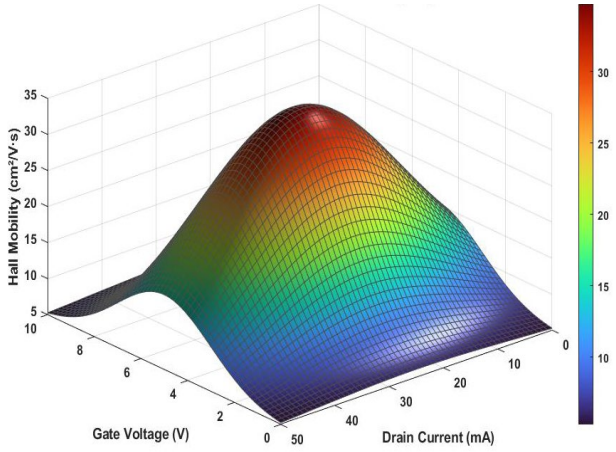

Fig. 8. 3D surface plot of hall mobility as a function of gate voltage and drain current.

These detailed analyses of Hall effect measurements and related electrical properties provide critical insights into the performance of ZnO thin films doped with boron and fluorine. The consistent trends across Figures 2 to 8 emphasize the significant improvements in electrical and optical properties through precise doping and optimization of operational parameters. A thorough comprehension of these properties is vital for the advancement of high-performance ZnO-based electronic and optoelectronic devices. Electrical characterization through Hall effect measurements demonstrated that the incorporation of B and F into ZnO significantly enhanced both charge carrier concentration and transport mobility. The highest carrier concentration was observed at a doping concentration of 3% B and 1% F, indicating an optimal doping level for enhancing the electrical properties of ZnO thin films. The increase in carrier concentration is attributed to the introduction of shallow donor states by boron and fluorine, which provide additional free carriers. This observation is consistent with earlier studies on the electrical properties of doped ZnO films [11, 13, 19].

4. Conclusions

This study underscores the significant enhancements in the structural, electrical, and optical properties of ZnO thin films through boron and fluorine co-doping. By leveraging advanced deposition techniques and comprehensive characterization, the research illuminates the underlying mechanisms by which B-F co-doping augments the performance of ZnO-based semiconductors. The results not only corroborate previous studies [3, 8, 14, 20] but also contribute to the advancement of next-generation optoelectronic devices. The precise optimization of doping concentrations is essential for achieving the targeted electrical, optical, and structural properties. These findings demonstrate that boron and fluorine co-doping in ZnO significantly enhances mobility, carrier concentration, and overall electrical conductivity. Such improvements make these thin films highly promising for diverse optoelectronic applications, including photodetectors, light-emitting diodes (LEDs), and solar cells [22,23]. The subsequent annealing process further enhanced the crystallinity and electrical characteristics of the films. X-ray diffraction (XRD) analysis revealed significant changes in crystallite size and lattice parameters due to B-F co-doping, indicating the successful incorporation of dopants into the ZnO lattice.

These structural modifications, including reduced crystallite size and increased lattice strain with higher doping concentrations, are critical for tuning the material's properties. Complementing these findings, scanning electron microscopy (SEM) offered detailed characterization of the surface morphology and grain structure of ZnO thin films. SEM analysis revealed a systematic reduction in grain size and an increase in surface roughness with increasing doping concentrations. These microstructural modifications are in strong agreement with the X-ray diffraction (XRD) results, further substantiating the critical role of dopant incorporation in modulating the structural integrity,

crystallinity, and defect landscape of ZnO thin films. Photoluminescence (PL) spectroscopy further highlighted the effects of B-F co-doping, showing notable shifts in emission peaks and variations in radiative recombination efficiency across different doping levels. The increased intensity of PL spectra with optimized doping levels indicates enhanced electron-hole recombination, which is crucial for optoelectronic applications. These optical property enhancements are consistent with the structural modifications observed in the XRD and SEM analyses. Hall effect measurements confirmed the improvement in electrical conductivity and carrier concentration with increasing B-F co-doping levels.

The results demonstrated a decrease in resistivity and an increase in carrier mobility and concentration, highlighting the effectiveness of B-F co-doping in enhancing the electrical properties of ZnO thin films. These electrical property improvements align with the observed changes in structural and optical properties. Overall, this comprehensive study provides valuable insights into the mechanisms by which boron and fluorine co-doping modifies the properties of ZnO thin films. The results underscore the potential of B-F co-doped ZnO thin films for high-performance optoelectronic applications, providing a foundation for further advancements in material optimization and device engineering. The systematic approach and detailed characterization presented in this work provide a solid foundation for optimizing the doping process and tailoring the properties of ZnO-based materials for specific applications.

Acknowledgements

The authors extend their sincere appreciation to the Fergana Polytechnic Institute for providing the necessary facilities and resources to carry out this research. Special thanks go to the research team and technical staff for their invaluable support and contributions to the experimental setup and characterization processes.

References

[1] Faraj, M. G., Ibrahim, K. International Journal of Polymer Science, Article ID 302843, (2011); https://doi.org/10.1155/2011/302843
[2] Raship, N. A., Tawil, S. N. M., Nayan, N., Ismail, K. Materials, 16(2392), (2023); https://doi.org/10.3390/ma16062392
[3] Mirzajonov, Z., Sulaymonov, K., Rakhmonov, T., Yusupov, F., Khidirov, D., Rakhimjonov, J., E3S Web of Conferences, 549(03013), (2024); https://doi.org/10.1051/e3sconf/202454903013
[4] Dai, Y., Xiong, J., Ge, Y., Cheng, B., Wang, L., Wang, P., Liu, Z., Yan, S., Zhang, C., Xu, X., Shi, Y., Cheong, S.-W., Xiao, C., Yang, S. A., Liang, S.-J., Miao, F. Nature Communications, 15, Article 1129, (2024); https://doi.org/10.1038/s41467-024-45318-8
[5] Anders, J., Kazimierczuk, M., Leedy, K., Miller, N., Cooper, T., Streby, M., Schuette, M. Applied Physics Letters, 116(25), Article 252105, (2020); https://doi.org/10.1063/5.0009676
[6] Gnenna, E., Khemiri, N., Kanzari, M. SN Applied Sciences, 2(174), Article 1971-5, (2020); https://doi.org/10.1007/s42452-020-1971-5
[7] Karakaya, S. Journal of Materials Science: Materials in Electronics, 29, 1628-1638, (2018); https://doi.org/10.1007/s10854-017-8352-x
[8] Salih, E. Y., Ramizy, A., Aldaghri, O., Mohd Sabri, M. F., Madkhali, N., Alinad, T., Ibnaouf, K. H., Eisa, M. H. Crystals, 12(1), 79, (2022). https://doi.org/10.3390/cryst12010079
[9] Sultanov, N. A., Mirzajonov, Z. X., Yusupov, F. T., Rakhmonov, T. I. East European Journal of Physics, (2), 309-314, (2024); https://doi.org/10.26565/2312-4334-2024-2-35
[10] Benyahia, K., Benhaya, A., Aida, M. S. Journal of Semiconductors, 36(10), 103001, (2015); https://doi.org/10.1088/1674-4926/36/10/103001

[11] Yusupov, F. T., Rakhmonov, T. I., Akhmadjonov, M. F., Madrahimov, M. M., Abdullayev, S. S. East European Journal of Physics, (3), 425-434, (2024); https://doi.org/10.26565/2312-4334-2024-3-51
[12] Anders, J., Kazimierczuk, M., Leedy, K., Miller, N., Cooper, T., Streby, M., Schuette, M. Applied Physics Letters, 116(25), Article 252105, (2020); https://doi.org/10.1063/5.0009676
[13] Sarkar, D., et al., Silicon, (2017); https://doi.org/10.1007/s12633-016-9478-3
[14] Smet, P.F., et al., The European Physical Journal Plus, (2014); https://doi.org/10.1140/epjp/i2014-14203-3
[15] Chen G.-J., et al. (201), RSC Advances; https://doi.org/10.1039/C8RA02011D
[16] N. Sultanov, Z. Mirzajonov, F. Yusupov, E3S Web of Conferences, 458, 01013 (2023); https://doi.org/10.1051/e3sconf/202345801013
[17] Khanam, B.R., et al., Journal of Materials Science: Materials in Electronics, (2024). https://doi.org/10.1007/s10854-023-10532-9
[18] Nagare, B.J., et al., Nanoscale Advances, (2020); https://doi.org/10.1039/D0NA00222A
[19] Vamathevan V., et al. (2002), RSC Advances; https://doi.org/10.1039/D2RA04972A
[20] Vallejo, W., et al., PubMed, (2020); https://doi.org/10.3390/nano10040752
[21] Nemma, N. M., Sadeq, Z. S., East European Journal of Physics, (3), 271-278, (2023). https://doi.org/10.26565/2312-4334-2023-3-24
[22] Debajyoti Das, Laxmikanta Karmakar, Journal of Alloys and Compounds, Volume 824, 2020, 153902, ISSN 0925-8388; https://doi.org/10.1016/j.jallcom.2020.153902.
[23] Ukita, S., Tajiri, T., Uchida, K. AIP Advances, 13(9), (2023); https://doi.org/10.7567/APEX.10.072101